Journal of
Antivirals & Antiretrovirals
ISSN: 1948-5964

Hussain et al., J Antivir Antiretrovir 2018, 10:3
DOI: 10.4172/1948-5964.1000177

Research Article Open Access

Penta-1,4-Diene-3-One Oxime Derivatives Strongly Inhibit the Replicase Domain of Tobacco Mosaic Virus: Elucidation Through Molecular Docking and Density Functional Theory Mechanistic Computations

Waqar Hussain[1], Muhammad Ali[2], Muhammad Sohail Afzal[2], Nouman Rasool[2,3]*

[1]Department of Computer Science, University of Management and Technology, Lahore, Pakistan
[2]Department of Life Sciences, University of Management and Technology, Lahore, Pakistan
[3]Dr Panjwani Center for Molecular Medicine and Drug Research, International Center for Chemical and Biological Sciences, University of Karachi, Karachi 75270, Pakistan

Abstract

Tobacco mosaic virus (TMV) is one of the major concerns to the farmers as it infects several crops of economic importance such as tomato. The mechanism of viral infection in host initiates on the entry of TMV in the host cell and production of a capping enzyme i.e. RNA polymerase. Replication of virus produces multiple mRNAs which further encodes multiple proteins including coat proteins, movement proteins and an RNA-dependent RNA polymerase (RdRp). In the present study, TMV replicase domain has been targeted using a set of novel penta-1,4-diene-3-one oxime derivatives bearing a pyridine moiety. To further assess the reactivity of these compounds against TMV, molecular orbital energy descriptors were calculated using Density Functional Theory (DFT) correlations. The pharmacokinetics and pharmacological properties have also been analysed as the crop yields are to be consumed by the humans. Results revealed that among the 16 derivatives of penta-1,4-diene-3-one oxime, compound C, J, O and P showed the highest inhibitory potential. Reactivity of these compounds was also high, however, only compound C showed effective pharmacokinetics and pharmacological properties. Based on these results, it is concluded that compound C can be used as a potent inhibitor against TMV and the yields produced by a crop will be safe to be consumed by humans.

Keywords: TMV; Replicase domain; Penta-1,4-diene-3-one oxime derivatives; Molecular docking; DFT

Introduction

Tobacco mosaic virus (TMV; genus **Tobamovirus**; family **Virgaviridae**) was the first virus that was discovered and crystallized in 1886. It is an extensively distributed and a most destructive phytopathogen with a wide host range relating to the family Solanaceae. TMV has 6.3 to 6.6 kb positive single-stranded RNA genome. The gRNA and sgRNAs contain m7GPPPG (5'-cap) and a 3'-terminal tRNA like structure accepting histidine [1].

TMV is known to encode at least four proteins [2]. The first two replication proteins, 124-132 kDa and 181-189 kDa, are translated directly from the genomic RNA (gRNA). The two other proteins, 28-31 kDa movement protein and 17-18 kDa coat protein translate from two different 3' co-terminal subgenomic RNAs (sgRNAs). Replication of TMV is cytoplasmic most certainly associated with the endoplasmic reticulum [1].

The virus is not transmitted through insect vectors, pesticides, therefore, cannot be used to cope with the infection. However, several other compounds have been investigated for their anti-viral activities. Most of these were used to enhance defence related gene expression. Fatty acids, like cottonseed oil, derived oleic acid promote moderate anti-TMV resistance in Nicotiana tabacum and **N. glutinosa** [3].

Several other anti-viral compounds have previously been investigated, like antofine alkaloids [4], azadirachtins [5], β-carboline alkaloids [6], gossypols [7], limonoids [8], rutins [9], and trans-ferulic acid derivatives containing acylhydrazone moiety [10]. However, the discovery of novel and potent inhibitors against TMV is still under consideration. In a recent study, TMV has been targeted using a series of novel penta-1,4-diene-3-one oxime ether derivatives bearing a pyridine moiety [11]. Keeping in view the economic importance of TMV, the 16 derivatives of penta-1,4-diene-3-one oxime ether are docked against the replicase domain of TMV, in this study. The reactivity of strongly inhibiting compounds is also analysed by calculating molecular orbital energy descriptors and their band energy gap. Furthermore, pharmacological properties and pharmacokinetics have also been analysed for the compounds.

Materials and Methods

Homology modelling

The current study targeted the TMV-RdRp protein to identify the potential of reported inhibitors by Wang et al., however, there was no crystal structure available for this protein. Due to this reason, homology modelling was performed to model the tertiary structure of the protein. The sequence of TMV-RdRp domain (UniProt Accession ID: P03586) was used for modelling. NCBI-BLAST was used to find the homologous proteins of TMV-RDRP and homology modelling was performed using Modeller 9.18 [12,13]. The Modeller initially built the profile and alignment of template and query sequence, and later on, based on this alignment, predicted the structure for query sequence.

Compound set

A total of 16 compounds were used for docking against TMV-

***Corresponding author:** Nouman Rasool, Department of Life Sciences, University of Management and Technology, Lahore, Pakistan, Tel: +923074449017 Email; nouman.rasool@umt.edu.pk

Received September 27, 2018; **Accepted** October 18, 2018; **Published** October 25, 2018

Citation: Hussain W, Ali M, Afzal MS, Rasool N (2018) Penta-1,4-Diene-3-One Oxime Derivatives Strongly Inhibit the Replicase Domain of Tobacco Mosaic Virus: Elucidation Through Molecular Docking and Density Functional Theory Mechanistic Computations. J Antivir Antiretrovir 10: 028-0034. doi:10.4172/1948-5964.1000177

RdRp, taken from a recent study in which TMV has been targeted using series of novel penta-1,4-diene-3-one oxime ether derivatives bearing a pyridine moiety [11]. The structures were drawn using ChemSketch [14]. Energy minimization and 3D structure optimization was carried out for all the compound structures using protocols defined in ACD ChemSketch.

Molecular docking and binding energy estimation

Molecular docking of TMV-RdRp with selected compounds was performed using Autodock Tools and Autodock Vina [15,16]. Using the Discovery Studio 2.5 software, CHARMM27 force field was applied onto the protein structure. Subsequently, steric overlaps were removed, and the structure were processed 1,000 steps using the smart-minimizer algorithm. Auto dock tools were used to prepare TMV-RdRp model by the addition of polar hydrogen bonds which optimized the interactions between inhibitors and TMV-RdRp. Torsion adjustment was performed for the ligands as the ligand needs information regarding torsion. This illustrates which torsions are to be treated as rotatable during the docking. Exhaustiveness was used as E=128 with smaller search spaces to find out the correct conformation. The three-dimensional grid was designed to define the search space within the receptor, focusing the binding pocket comprised of the catalytic site. The volume of the grid was 22 x 22 x 30 Å3. For all compounds, interactions were analysed and binding energies were calculated using Autodock Vina. Moreover, Ki was calculated as=Δ (1) where ΔG represents the binding free energy, R (gas constant) has a value of 1.9872cal/mol while T (temperature) has a value of 298.15k.

DFT analysis

To study the reactivity and efficiency of the compounds against TMV-RdRp, molecular orbital energy descriptors were calculated such as Highest Occupied Molecular Orbital (HOMO) and Lowest Unoccupied Molecular Orbital (LUMO) energy using a DFT-based analysis by applying the Becke3-Lee-Yang-Parr (B3LYP) correlation function of DFT [17,18]. The band energy gap (ΔE) was calculated using the expression. The energy calculations were made using ORCA program [19].

The ADMET and drug likeness prediction

Compounds were filtered on the basis of Absorption, Distribution, Metabolism, Excretion and Toxicity (ADMET) studies and drug-likeness prediction, using the PreADMET server [20]. Compounds were assessed for the Solubility (ESOL), Gastro-Intestinal (GI) absorption, Blood Brain Barrier (BBB) penetration, Lipinski's rule of five and their toxicity.

Results

The tertiary structure of TMV RdRp domain

The tertiary structure of TMV-RdRp domain was modelled through Modeller9.19, due to unavailability of the crystal structure. For searching homologous templates, BLAST was used, and results indicated that RdRp from human rhinovirus serotype 14 (PDB ID: 1XR5) was maximum homologous with TMV-RdRp. Based on the template, 10 models were generated and among those 10 models, a structure with lowest discrete optimized protein energy (DOPE) and highest GA341 assessment score i.e. -16121.53711 and 0.07650, respectively, were considered for further processes. For the refinement of the model, ModRefiner server was used which performed the atomic-level, high-resolution protein structure refinement [21]. The refined tertiary structure was comprised of 8 α-helices and 5 β-strands (Figure 1).

Molecular Docking

Active site was identified prior to the docking process. To verify the active site regions in TMV replicase, ClustalW alignment was performed using the sequences of TMV replicase, Rehmannia mosaic virus, and Potato virus X (strain X3). The conserved domain is found at GDDS amino acid motif in all these sequences. The binding site residues were found to be Asp7, Ile8, Ser9, Lys10, Tyr11, Asp12, Arg64, Ser66, Thr71, Asn75, Gly99, Asp100, Asp101, and Lys128. From these studies, GDD motif is chosen to be the active site region for RNA-dependent RNA polymerase domain of TMV replicase. All the 16 compounds are docked against the TMV-RdRp (Table 1).

Among the 16 derivatives, compound C, J, O and P showed the highest inhibitory potential. Compound C docked with binding affinity -9.3 kcal/mol (Ki =0.15 μM), greater than affinities of all other compounds and interacted with Lys94 and Ala96 (Figure 2).

Compound J docked with binding affinity -9.2 kcal/mol (Ki=0.18 μM) and interacted with Lys94 and Ala96, Asp100, Asp101 and Leu103. Compound O docked with binding affinity -9.1 kcal/mol (Ki=0.21 μM) and interacted with Lys94 and Ala96, Asp100 and Leu103. Compound P docked with binding affinity -9.0 kcal/mol (Ki=0.25 μM) and interacted with Cys98 and Asp101, Ser102, Tyr105 and Pro107. Remaining compounds docked with lower binding affinities, ranged from -8.9 kcal/mol (Ki=0.29 μM) to -6.8 kcal/mol (Ki=10.23 μM). The compounds were taken from a study by Wang et al. and the results are in accordance with the present study.

Reactivity analysis of penta-1,4-diene-3-one derivatives

For analysing the reactivity of docked compounds in the binding pocket of TMV-RdRp, compounds and the binding pocket residues was the point of interest for energy calculations. Results revealed that compound C was most reactive compound within the binding pocket of RdRp as band energy gap was narrow as compared to others i.e. 0.119 eV (Table 2).

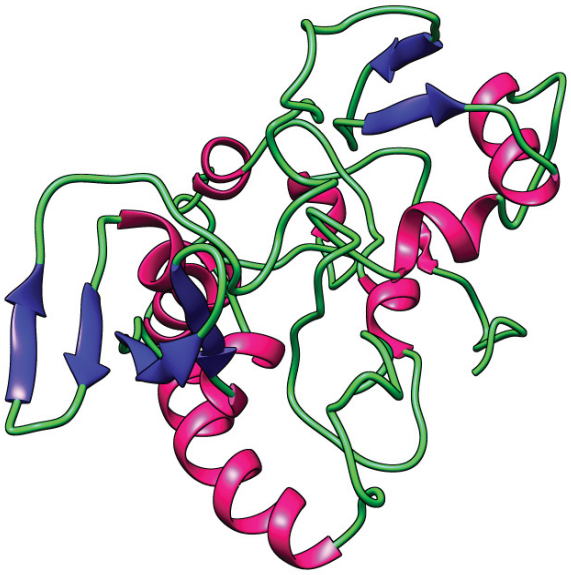

Figure 1: Predicted tertiary structure of TMV-RdRp. Magenta represents the α-helices and blue represents the β-strands while green is for random coil.

Compound	Interacting Residues	Binding affinity (kcal/mol)	K_i (μM)
C	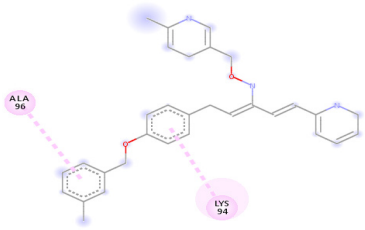	-9.3	0.15
J	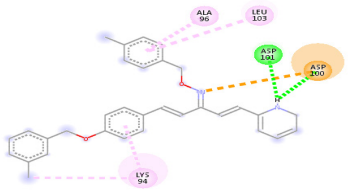	-9.2	0.18
O	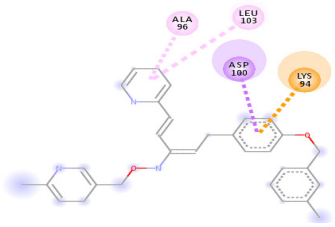	-9.1	0.21
P	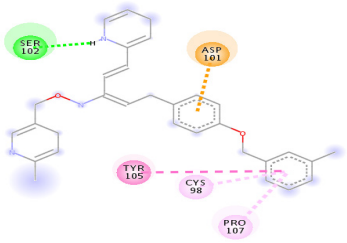	-9.0	0.25
G	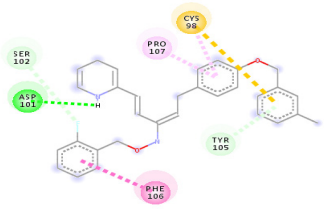	-8.9	0.29
L	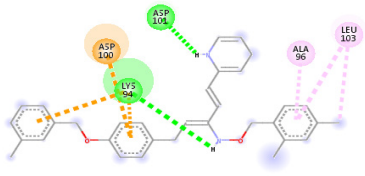	-7.9	1.60

D	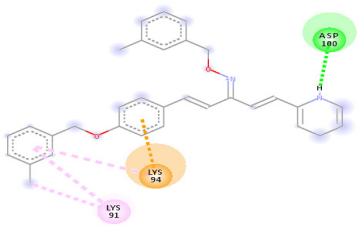	**-7.8**	1.89
M	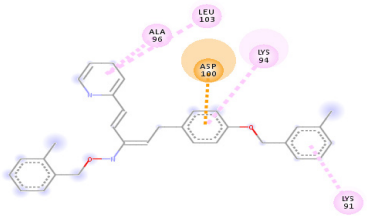	**-7.7**	2.24
I	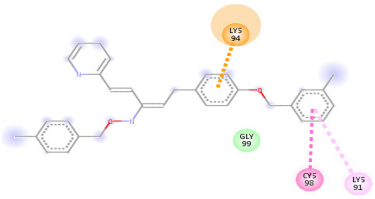	**-7.6**	2.65
E	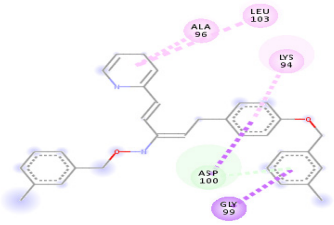	**-7.5**	3.14
N	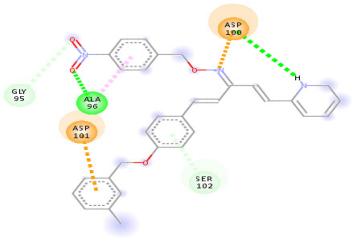	**-7.4**	3.71
K	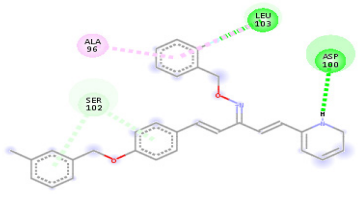	**-7.3**	4.40

B	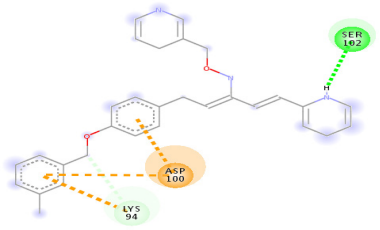	-7.2	5.21
F	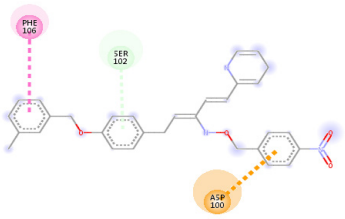	-7.2	5.21
A	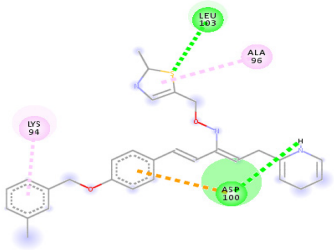	-7.1	6.16
H	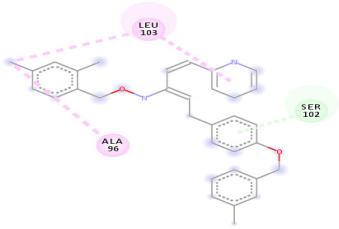	-6.8	10.23

Table 1: Docking of 16 penta-1,4-diene-3-one oxime derivatives against TMV-RdRp.

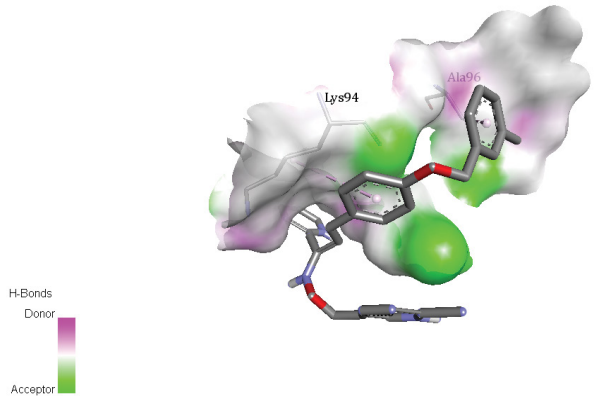

Figure 2: Interaction of Compound C with the binding pocket of TMV-RdRp (binding affinity -9.3 kcal/mol, Ki =0.15 μM).

Compounds	E_{LUMO} (kcal/mol)	E_{HOMO} (kcal/mol)	Band energy gap (ΔE) (kcal/mol)
C	-0.186	-0.305	0.119
J	-0.295	-0.417	0.122
O	-0.269	-0.393	0.124
P	-0.220	-0.346	0.126
G	-0.157	-0.305	0.148
L	-0.158	-0.306	0.148
D	-0.237	-0.387	0.150
M	-0.188	-0.339	0.151
I	-0.180	-0.332	0.152
E	-0.227	-0.379	0.152
N	-0.131	-0.290	0.159
K	-0.195	-0.360	0.165
B	-0.256	-0.419	0.163
F	-0.252	-0.417	0.165
A	-0.285	-0.455	0.170
H	-0.162	-0.333	0.171

Table 2: Band energy gaps analysis of compounds in the binding pocket of TMV-RdRp.

Pharmacological properties and pharmacokinetics of the compounds

Pharmacological assessment of the compounds was necessary

Compounds	ESOL Class	GI absorption	BBB permeant	Lipinski violations	Rodent Test	Ames Test	Carcinogenic
A	Moderately soluble	Low	No	1	Non Toxic	Non Toxic	Non Carcinogenic
B	Soluble	High	No	0	Non Toxic	Non Toxic	Non Carcinogenic
C	Soluble	High	No	0	Non Toxic	Non Toxic	Non Carcinogenic
D	Moderately soluble	Low	No	1	Non Toxic	Non Toxic	Non Carcinogenic
E	Moderately soluble	Low	No	1	Non Toxic	Non Toxic	Non Carcinogenic
F	Moderately soluble	Low	No	1	Non Toxic	Non Toxic	Non Carcinogenic
G	Moderately soluble	Low	No	1	Non Toxic	Non Toxic	Non Carcinogenic
H	Moderately soluble	Low	No	2	Non Toxic	Non Toxic	Non Carcinogenic
I	Moderately soluble	Low	No	1	Non Toxic	Non Toxic	Non Carcinogenic
J	Moderately soluble	Low	No	2	Non Toxic	Non Toxic	Non Carcinogenic
K	Moderately soluble	Low	No	1	Non Toxic	Non Toxic	Non Carcinogenic
L	Moderately soluble	Low	No	2	Non Toxic	Non Toxic	Non Carcinogenic
M	Moderately soluble	Low	No	2	Non Toxic	Non Toxic	Non Carcinogenic
N	Moderately soluble	Low	No	2	Non Toxic	Non Toxic	Non Carcinogenic
O	Moderately soluble	Low	No	1	Non Toxic	Non Toxic	Non Carcinogenic
P	Moderately soluble	Low	No	1	Non Toxic	Non Toxic	Non Carcinogenic

Table 3: Pharmacological assessment of penta-1,4-diene-3-one derivatives.

as the passing compounds would not cause any lethal effects during consumption of crop yields by a human. All the 16 derivatives were analysed for their pharmacological properties and pharmacokinetics. Properties being analysed included solubility, gastrointestinal (GI) absorption, blood-brain barrier (BBB) permeability, Lipinski's rules violation and toxicity. The criteria set for selecting suitable compounds were: (BBB-permeability=Yes) & (Solubility = High) & (GI-absorption=High) & (Lipinski's violations=0) & (Toxicity=No)

At each level of criteria set, the number of compounds selected for further analysis was reduced. Among all the compounds, compound B and C passed the criteria while the other 14 compounds violated the criteria (Table 3).

Discussion

In the present study, RdRp domain of TMV is targeted to control the TMV infection in plants as this virus infect several crops of economic importance and is one of the major concerns of farmers [22]. RdRp is an important biological target for inhibition of TMV complex as this domain provides the catalytic activity for the synthesis of TMV RNA and mediates the replication of TMV [23]. Here, a set of compounds reported by Wang et al. is docked against TMV-RdRp to identify the potential ligand that could inhibit the catalytic domain of TMV replicase [11]. The inhibitory potential of these small molecules is also analysed in terms of reactivity through post-docking quantum mechanistic calculations to identify the small molecules that target a much larger RdRp domain involving catalytic region amino acid residues (GDD) [24].

Among the 16 derivatives, compound C, J, O and P showed the highest inhibitory potential. Compound C docked with binding affinity -9.3 kcal/mol (Ki=0.15 μM), greater than affinities of all other compounds. Wang et al., reported that according to the results of bioassays, several compounds elucidated good antiviral activities against TMV and the compounds C, J, O and P showed highest curative activities among all the others against TMV, with EC50 values of 274.8, 299.2, 251.8 and 287.7 μg/mL, respectively [11].

In literature, no study has been reported previously targeting the analysis of compound reactivity within the binding pocket of TMV proteins. However, DFT based analysis is reported in some other studies and the band energy gaps of the present study are also within the same range as those reported in previous studies [25-27]. The lower band energy gap reflects higher reactivity of compounds as the ELUMO and EHOMO are responsible for the charges transferred in a chemical reaction [28]. In the present study, the compounds were evaluated based upon DFT analysis and the lower band energy gap of molecular orbital energies illustrated the higher reactivity of these compounds, validating the potential of these compounds against RdRp [29].

Pharmacological assessment of the compounds was necessary as the passing compounds would not cause any lethal effects during consumption of crop yields by a human. All the 16 derivatives were analysed for their pharmacological properties and pharmacokinetics. Properties being analysed included solubility, gastrointestinal (GI) absorption, blood-brain barrier (BBB) permeability, Lipinski's rules violation and toxicity. Among all the compounds, compound B and C passed the criteria while the other 14 compounds violated the criteria.

These all parameters are necessary to evaluate the drug-likeness of a compound and helps in assessing the effective disposition of compounds in the human body. It is well established in the literature that a drug should not reach the central nervous system (CNS) by penetrating through BBB [30]. The solubility is considered to be one of the key physical descriptors of a drug regarding the determination of its effectiveness, whereas high GI absorption reflects the effective plasma concentration profile of oral administration in humans [31,32]. Lipinski's rule of five is known as a rule of thumb to evaluate the drug-likeness of a compound which is based on lipophilicity, molecular weight and the hydrogen donor-acceptor bonds [33].

Computational approaches for drug development are proven to be effective and time efficient as these are not based on costly and hectic laborious works. In drug discovery, the molecular dynamics simulations help in the study of the motions of biological macromolecules such as proteins and nucleic acids. Computational mechanisms of biological targets and their associated small-molecule ligands can play an important role in drug discovery; including the identification of binding sites, virtual screening of numerous compounds libraries and estimation of ligand binding energies. The docking of inhibitors with the enzymes elucidate the mechanism of inhibition along with the specificity and efficiency of that inhibitor. Based on results it is

concluded that compound C can be considered as a most effective inhibitor against TMV as it docked with a high binding affinity with high reactivity and showed effective pharmacological properties and pharmacokinetics.

Compliance with Ethical Standards

Funding

No funding was received for this study.

Conflict of Interest

The authors declare no conflict of interest.

Research Involving Human Participants and/or Animals

The authors declare that no human participants or animals were involved in this study.

References

1. Adams MJ, Adkins S, Bragard C, Gilmer D, Li D, et al. (2017) ICTV Virus Taxonomy Profile: Virgaviridae. J Gen Virol 98: 1999-2000.
2. Ali M (2016) Towards a coherent nomenclature of plant viruses. Virol Sin 3: 197-198.
3. Zhao L, Chen Y, Wu K, Yan H, Hao X, et al. (2017) Application of fatty acids as antiviral agents against tobacco mosaic virus. Pest Biochem Physiol 139: 87-91
4. Wang ZW, Wei P, Xu XZ, Liu YX, Wang LZ, et al. (2012) Design, Synthesis, and Antiviral Activity Evaluation of Phenanthrene-Based Antofine Derivatives. J Agri Food Chem 60: 8544-8551.
5. Fan HD, Zhang CH, Yan SJ, Lin J (2009) Advances of synthesis and structure modification and bioactivity of Azadirachtin. Chin J Org Chem 1: 20-33.
6. Song HJ, Liu YX, Liu YX, Huang YQ, Li YQ, et al. (2014) Design, synthesis, anti-TMV, fungicidal, and insecticidal activity evaluation of 1,2,3,4-tetrahydro-β-carboline-3-carboxylic acid derivatives based on virus inhibitors of plant sources. Bioorg Med Chem Lett 24: 5228-5233.
7. Li L, Li Z, Wang K, Zhao S, Feng J, et al. (2014) Design, synthesis, and biological activities of aromatic Gossypol Schiff base derivatives. J Agri Food Chem 62: 11080-11088.
8. Ge YH, Liu KX, Zhang JX, Mu SZ, Hao XJ (2012) The Limonoids and Their Antitobacco Mosaic Virus (TMV) Activities from Munronia unifoliolata Oliv. J Agri Food Chem 60: 4289-4295.
9. Han Y, Ding Y, Xie D, Li P, Li X, et al. (2015) Design, synthesis, and antiviral activity of novel rutin derivatives containing 1, 4-pentadien-3-one moiety. Eur J Med Chem 92: 732-737.
10. Wang Z, Xie D, Gan X, Zeng S, Zhang A, et al. (2017) Synthesis, antiviral activity, and molecular docking study of trans-ferulic acid derivatives containing acylhydrazone moiety. Bioorg Med Chem Lett 27: 4096-4100.
11. Wang X, Chen M, Li Q, Zhang J, Ruan X, et al. (2017) Synthesis and antiviral activities of novel penta-1, 4-diene-3-one oxime derivatives bearing a pyridine moiety. Chem Pap 71: 1225-1233
12. Johnson M, Zaretskaya I, Raytselis Y, Merezhuk Y, McGinnis S, et al. (2008) NCBI BLAST: a better web interface. Nuc Acids Res 36: W5-W9.
13. Webb B, Sali A (2014) Comparative protein structure modeling using Modeller. Curr Protoc Prot Sci 47: 1-32.
14. ACD/ChemSketch (2015) Advanced Chemistry Development, Inc. Toronto, ON, Canada.
15. Morris GM, Huey R, Olson AJ (2008) Using autodock for ligand□receptor docking. Curr Protoc Bioinfo 8: 8-14.
16. Trott O, Olson AJ (2010) AutoDock Vina: improving the speed and accuracy of docking with a new scoring function, efficient optimization, and multithreading. J Comp Chem 31: 455-61.
17. Gill PM, Johnson BG, Pople JA, Frisch MJ (1992) The performance of the Becke—Lee—Yang—Parr (B—LYP) density functional theory with various basis sets. Chem Phy Lett 197: 499-505.
18. Qaddir I, Rasool N, Hussain W, Mahmood S (2017) Computer-aided analysis of phytochemicals as potential dengue virus inhibitors based on molecular docking, ADMET and DFT studies. J Vec Borne Dis 54: 255-262.
19. Neese F (2012) The ORCA program system. Wiley Interdisciplinary Reviews: Comp Mol Sci 2: 73-78.
20. Lee SK, Park SH, Lee IH, No KT (2007) PreADMET Ver. 2.0, BMDRC: Seoul. Korea.
21. Schmatulla A, Maghelli N, Marti O (2007) Micromechanical properties of tobacco mosaic viruses. J Microscop 225: 264-268.
22. Osman TA, Buck KW (1996) Complete replication in vitro of tobacco mosaic virus RNA by a template-dependent, membrane-bound RNA polymerase. J Virol 70: 6227-6234.
23. Xu D, Zhang Y (2011) Improving the physical realism and structural accuracy of protein models by a two-step atomic-level energy minimization. Biophy J 101: 2525-2534.
24. Dunigan DD, Zaitlin M (1990) Capping of tobacco mosaic virus RNA: Analysis of viral-coded guanylyltransferase-like activity. J Biol Chem 265: 7779-7786.
25. Kavitha R, Karunagaran S, Chandrabose SS, Lee KW, Meganathan C (2015) Pharmacophore modeling, virtual screening, molecular docking studies and density functional theory approaches to identify novel ketohexokinase (KHK) inhibitors. BioSystems 138: 39-52.
26. Gogoi D, Baruah VJ, Chaliha AK, Kakoti BB, Sarma D, et al. (2017) Identification of novel human renin inhibitors through a combined approach of pharmacophore modelling, molecular DFT analysis and in silico screening. Comput Biol Chem 69: 28-40.
27. Rasool N, Iftikhar S, Amir A, Hussain W (2018) Structural and quantum mechanical computations to elucidate the altered binding mechanism of metal and drug with pyrazinamidase from Mycobacterium tuberculosis due to mutagenicity. J Mol Graph Model 80: 126-131.
28. Eroglu E, Türkmen H (2007) A DFT-based quantum theoretic QSAR study of aromatic and heterocyclic sulfonamides as carbonic anhydrase inhibitors against isozyme, CA-II. J Mol Graph Model 26: 701-708.
29. Ai C, Li Y, Wang Y, Li W, Dong P, et al. (2010) Investigation of binding features: effects on the interaction between CYP2A6 and inhibitors. J Comput Chem 31: 1822-1831.
30. Tran N (2011) Blood-Brain Barrier. Encyclopaedia of Clinical Neuropsychology Springer New York.
31. Kimura T, Higaki K (2002) Gastrointestinal transit and drug absorption. Biol Pharm Bull 25: 149-164.
32. Delaney JS (2004) ESOL: estimating aqueous solubility directly from molecular structure. J Chem Inf Comput Sci 44: 1000-1005.
33. Lipinski CA, Lombardo F, Dominy BW, Feeney PJ (1997) Experimental and computational approaches to estimate solubility and permeability in drug discovery and development settings. Adv Drug Deliv Rev 46: 3-26.